Planta (2007) 226:267–281
DOI 10.1007/s00425-007-0479-1

ORIGINAL ARTICLE

Studies of xylan interactions and cross-linking to synthetic lignins formed by bulk and end-wise polymerization: a model study of lignin carbohydrate complex formation

Abdellatif Barakat · Heiko Winter · Corinne Rondeau-Mouro · Bodo Saake · Brigitte Chabbert · Bernard Cathala

Received: 26 October 2006 / Accepted: 3 January 2007 / Published online: 1 March 2007

Abstract The mechanism of lignin carbohydrate complex formation by addition of polysaccharides on quinone methide (QM) generated during lignin polymerisation was investigated using a model approach. Dehydrogenation polymers (DHPs, lignin model compounds) were synthesized from coniferyl alcohol in the presence of a glucuronoarabinoxylan (GAX) extracted from oat spelts, by Zutropfverfahren (ZT) and Zulaufverfahren (ZL) methods. The methods ZT and ZL differed in their distribution of QM over the reaction period but generated roughly the same QM amount. Steric exclusion chromatography of the ZT and ZL reaction products showed that only the ZT reaction produced high molar mass compounds. Covalent linkages in the ZT reaction involving ether bonds between GAX moiety and α carbon of the lignin monomer were confirmed by ^{13}C NMR and xylanase-based fractionation. The underlying phenomena were further investigated by examining the interactions between GAX and DHP in sorption experiments. GAX and DHPs were shown to interact to form hydrophobic aggregates. In the ZT process, slow addition permitted polymer reorganisation which led to dehydration around the lignin-like growing chains thereby limiting the addition of water on the quinone methide formed during polymerisation and thus favoured lignin–carbohydrate complex (LCC) formation.

Keywords Aggregation · Carbohydrate complex · Dehydrogenation polymers (DHP) · Glucuronoarabinoxylan · Lignin

Abbreviations

CA	Coniferyl alcohol
CPMAS	Cross polarization magic angle spinning
DHP	Dehydrogenation polymer
DMSO	Dimethyl sulfoxide
GAX	Glucuronoarabinoxylan
HPAEC	High-pressure anion exchange chromatography
LCC	Lignin–carbohydrate complex
LiBr	Lithium bromide
NMR	Nuclear magnetic resonance
QM	Quinone methide
SEC	Steric-exclusion chromatography
ZL	Zulaufverfahren
ZT	Zutropfverfahren

A. Barakat · B. Chabbert
Unité Mixte de Recherche Fractionnement des AgroRessources et Emballages, Institut National de la Recherche Agronomique, Equipe Parois et Matériaux Fibreux, 51686 Reims Cedex 2, France

H. Winter · B. Saake
Federal Research Centre for Forestry and Forest Products, Institute for Wood Chemistry and Chemical Technology of Wood, Leuschnerstr. 91, 21031 Hamburg, Germany

C. Rondeau-Mouro · B. Cathala (✉)
Unité Biopolymères, Interactions et Assemblages, Institut National de la Recherche Agronomique, Rue de la géraudière, 44316, BP 71627, Nantes Cedex 3, France
e-mail: cathala@nantes.inra.fr

Introduction

Lignified plant cell wall is formed by successive deposition of cellulose, hemicelluloses and lignins to form a composite in which component polymers are physically and chemically bound to each other. This mechanism of biogenesis is important in determining the ultrastructure of

lignified plant cell walls and thus their physical and chemical properties. Cell wall formation ended by lignin deposition according to the dehydrogenative polymerisation of monolignols (*p*-coumaryl, coniferyl and sinapyl alcohols, Fig. 1; Terashima et al. 1993). Lignin polymerisation therefore occurs within a water swollen polysaccharide gel. During this process, polysaccharides and lignin are covalently linked through lignin–carbohydrate complexes, as demonstrated several decades ago by Björkman (1957). These covalent links are important in the biological roles of plant cell walls (mechanical resistance, protection against pathogens) and in the ability of the cell wall to be transformed for application purposes (production of pulp or chemicals, biodegradation, etc). Comprehension of the interactions between lignin and polysaccharides and their formation processes may therefore be helpful in understanding cell wall architecture. Such information could also be used to improve the fractionation and transformation of cell-wall-related products.

Two main processes are involved in the mechanism of lignin–carbohydrate complex (LCC) formation. The first is based on oxidative coupling of the phenolic components of the plant cell wall (Fry 1986; Grabber et al. 2000). The polymerisation of monolignols in the presence of feruloylated polysaccharides, for example, has been described as a very efficient way of coupling polysaccharides to the lignin network (Grabber et al. 2000, 2002). These processes are restricted to herbaceous species and are thought to occur in

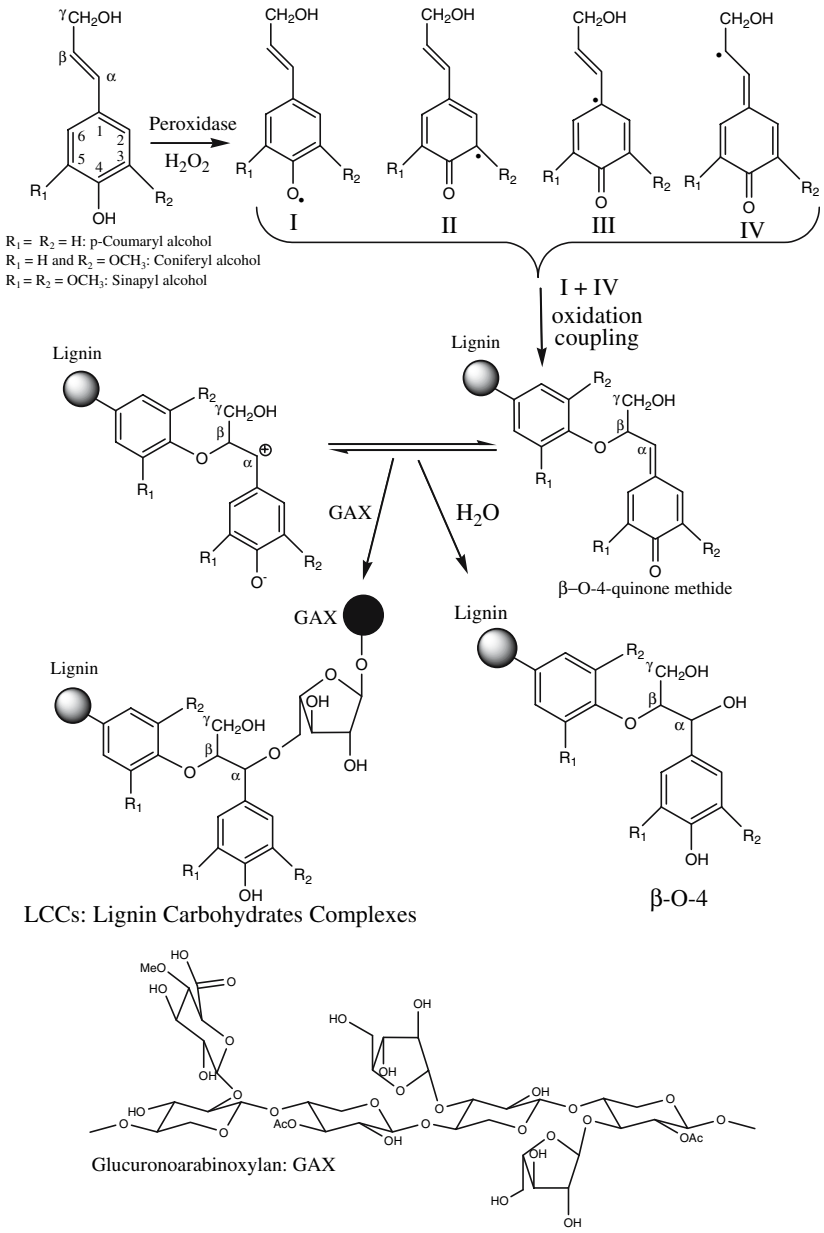

Fig. 1 Addition of nucleophiles to the quinone methide intermediate generated during the dehydrogenation of coniferyl alcohol. Addition of water will form the *β-O*-4 linkages whereas addition of polysaccharide will form lignin–carbohydrate complex. Thus, LCC formation competes with *β-O*-4 formation. In hydrated media the latter process will be prominent

the early stages of lignification. The second process, ubiquitous in all lignified walls, involves the addition of nucleophilic groups on the transient quinone methide (QM) intermediate generated during the oxidative polymerisation of lignin (Takahashi and Koshijima 1988; Xi et al. 2000; Terashima 2001; Fig. 1). Studies on cell wall materials have indicated that these linkages represent a non negligible part of the lignin unit (Terashima 2001). However, the complete process of LCC formation is not fully understood since many nucleophiles (i.e. hydroxyl or carboxylic groups of hemicelluloses, phenols, water) are present in the cell wall. Due to their similar nucleophilic potentials, competition based on ratio concentration may occur between them. Some works based on model studies have demonstrated this competition and emphasized the fact that the addition of hemicellulose to quinone methide may be limited by competition of the water addition. For instance, the addition of neutral monomeric sugar to QM does not occur even in a buffered 1:3 dioxane solution containing ten equivalents (compared to QM) of methyl α-D-glucopyranoside (Sipilä 1990). Thus, to displace the reaction in favour of LCC formation, several authors increased the reaction duration and temperature (Hemmingson and Leary 1975), or limited the water concentration either by introducing aqueous/organic solvent mixtures (Sipilä 1990) or high saccharide concentrations (Tanaka et al. 1976) which suggests that nonaqueous conditions are necessary for LCC formation. All these hypotheses show some consistency with the cell wall conditions during lignification. However, other model studies have shown that LCC can be formed in a dilute aqueous solution of hemicelluloses (Ohnishi et al. 1992; Cathala and Monties 2001). The present work develops the hypothesis that LCC formation is not only under the kinetic control of water/polysaccharide competition. Local structural heterogeneities may also affect this process such as the formation of aggregates stabilized by noncovalent interactions between hemicelluloses and lignin. These supramolecular structures change the local environment of the reaction by lowering the local water concentration and thus affect (or control) the LCC formation.

In the present study, dehydrogenation polymers (DHPs, lignin model compounds) were synthesized in the presence of a glucuronoarabinoxylan (GAX) extracted from oat spelts, since GAX is the major hemicellulose present in angiosperms. The GAX sample used in this study was free of phenolic acids and permitted focus on the QM pathway of LCC formation. DHPs were synthesised according to the Zulaufverfahren (ZL) and Zutropfverfahren (ZT) methods. The first one consists in the simultaneous adding of all reactants whereas, in the later one, reagents are slowly added. The major difference between ZL and ZT polymerisation lies in the distribution of the radical over the reaction period. All other physicochemical parameters remain identical in both methods, notably the amounts of quinone methide generated during the reactions. This comparison can be used to evaluate the competition occurring between water and polysaccharide. Steric-exclusion chromatography (SEC) analysis of the ZL and ZT reaction mixtures revealed the formation of a high molar mass product in ZT only. The occurrence of covalent linkages in the ZT products was confirmed by NMR and xylanase-based fractionation, and indicated that LCC formation was not only under kinetic control. We also demonstrated that interactions between GAX and DHP resulted in the formation of hydrophobic micro-domains.

Materials and methods

Extraction and purification of oat spelt GAX

The GAX sample was produced by successive extraction and fractionation (Winter et al. 2006). The starting material was extracted from oat spelts with 5% (w/v) NaOH at 90°C and purified by washing with methanol/water (60/40 v/v), methanol and ether. The purified sample was bleached with 3% ClO_2 at 70°C and 25% concentration (w/w) for 3 h, dissolved in water (concentration 5% w/v; 100°C for 20 min, shaken over night at 20°C) and centrifuged (20 min, 2,800 *g*) to remove the insoluble fraction. The supernatant was freeze dried (Alpha 2-4 LSC, Christ, Osterode am Harz, Germany), and yielded the water-soluble fraction GAX. The physicochemical characteristics of this fraction are presented in Table 1.

Synthesis of unlabelled and labelled coniferyl alcohol (4-hydroxy-3-methoxy cinnamyl alcohol)

Coniferyl alcohol was obtained using the procedure described by Ludley and Ralph (1996). Synthesis of $\alpha^{13}C$

Table 1 Physicochemical characteristics of oat spelt glucuronoarabinoxylan

Sugars composition (%)	Glucuronoarabinoxylan
Uronic acids	6.2
Ara	15.1
Xyl	64.7
Gal	5.5
Glc	4.5
Ara/Xyl	0.23
Mw (g/mol)	43000

Ara Arabinose, *Xy* xylose, *Ga* galactose, *Glc* glucose, *Ara/Xyl* molar ratio of L-arabinose to D-xylose, *Mw* weight average molar mass equivalent to pullulan standards

coniferyl alcohol was achieved according the previously published synthesis (Terashima 1996). Spectra of labelled and nonlabelled product were identical. ^{1}H NMR ($CDCl_3$, 250 MHz), 6.89 (m, 3H), 6.53 (d, 1H), 6.21 (d, 1H), 4.18 (d, 2H), 3.85 (s, 3H).

Polymerisation of coniferyl alcohol in glucuronoarabinoxylan solution

In both ZT and ZL, the DHPs were prepared with and without (control) GAX. Control DHPs were used for the sorption experiment and physical mixture. Three solutions were prepared for the polymerisation experiments. Solution A 100 mg of GAX dissolved in 100 ml of phosphate buffer (1/30 N; pH 5.0). Solution B 100 mg of coniferyl alcohol labelled or unlabelled (0.56 mmol) in 3 ml of dioxane and 22 ml of GAX (1 g/l) in phosphate buffer (1/30 N; pH 5.0). Solution C 0.1 ml (2 eq compared to coniferyl alcohol) of hydrogen peroxide H_2O_2 (35% wt in water) in 25 ml of GAX (1 g/l) in phosphate buffer (1/30 N; pH 5.0). For the end-wise polymerisation, ZT method, solutions B and C were gradually added to 50 ml of solution A, containing 5 mg of peroxidase (EC 1 11.1.7, 250–330 unit/mg, purchased from Sigma), for 4 h at 25°C. For the ZL method, all reagents were added simultaneously to 50 ml of solution A containing 5 mg of peroxidase. The reaction mixture was stirred for 4 h at 25°C. DHP controls without GAX were prepared in phosphate buffer (1/30 N; pH 5.0).

The concentrations of all the reagents in the ZL and ZT experiments are reported in Table 2. The total concentrations of QM able to react with water or GAX were estimated from the β-*O*-4 contents of ZL and ZT products synthesized under similar conditions (Cathala et al. 1998).

Monosaccharide composition determination

The neutral and acidic carbohydrates were identified and quantified by high-pressure anion exchange chromatography (HPAEC). Samples were hydrolysed with 12 M H_2SO_4 acid for 2 h at room temperature, then diluted at 1.5 M and allowed to react for 2 h at 100°C. All samples were then filtered (0.45 µm) before injection onto a CarboPac PA-1 anion exchange column (4 × 250 mm, Dionex, Voisins les bretonneux, France). Monosaccharide composition was analysed and quantified using L-fucose as the internal standard and standard solutions of neutral carbohydrates (L-arabinose, D-glucose, D-xylose, D-galactose) and uronic acids (D-galacturonic and D-glucuronic acids).

NMR spectroscopy

Solid-state NMR experiments were performed on a Bruker DRX 400 spectrometer (100.62 MHz for carbons; Wissenbourg, France). The CPMAS (cross polarization magic angle spinning) experiments were performed using a double resonance H/X CP-MAS 4 mm probe at a spinning rate of 10,000 Hz. The pulse sequence operated with a 3.75 µs 90° proton pulse, a 1 ms contact time at 62.5 kHz, a 3 s recycle time for an acquisition time of 34 ms during which dipolar decoupling (TPPM) was applied at 67 kHz. 1,024 scans were acquired at ambiant temperature (294 ± 1 K) and no line broadening was applied in order to perform the spectral decomposition. Chemical shifts were calibrated with external glycin, (carbonyl carbon at 176.03 ppm). The software used to decompose each spectrum was based on the SIMPLEX method (Lorentzian/Gaussian 50/50 line type).

Liquid-state NMR spectra were recorded on a Bruker ARX 400 spectrometer operating at a carbon frequency of 100.62 MHz. The NMR experiments were realized in DMSO-d_6 using a single pulse detection of carbon with power-gated ^{1}H decoupling. The 90° carbon pulse was set to 11.25 µs and a proton decoupling (WALTZ16) of 3 kHz was applied during acquisition (1.25 s) but also during the recycle delay (5 s) in order to gain signal by nuclear-overhauser enhancement (NOE; Kuhlmann and Grant 1968). Each NMR experiment was realized at 313 K with 22 K scans and calibration of the carbon chemical shifts were realised using the carbon signal of DMSO as an internal reference.

Table 2 Total concentration of CA, QM and arabinose and concentration ratio of the reactants calculated at the maximum of their concentration in the GAX–DHP ZL and GAX—DHP ZT reaction

	GAX–DHP ZL reaction	GAX–DHP ZT reaction
Total coniferyl alcohol concentration (mM)	2.77	2.77
Total QM concentration (mM) (based on β-*O*-4 content ZL 12%; ZT 15% determined by thioacidolysis (Cathala et al. 1998)	3.3	0.416
Xylose + arabinose monomers concentration (mM)	0.312	0.312
[GAX]/[QM] at the maximum concentration of QM (i.e. at t = 0 for ZL and after 3 min for ZT)	9.45	182
$[H_2O]^a$/[QM]	16.6×10^3	3.179×10^6

[a] $[H_2O]$ = 55 M

Size exclusion chromatography in dimethyl sulfoxide (DMSO)/water (9/1 v/v) containing 50 mM of LiBr

Analysis was performed using a multi-detection system consisting of a UV-Detector (LC 1200 UV/VIS-detector, Polymer Laboratories, Marseille, France), and a RI-detector (Shodex RI-71, Sopares, Gentilly, France). A set of GRAM columns from Polymer Standard Service (Mainz, Germany) was used (3, 100, 300 nm, each 8 × 300 mm). The eluent was a mixture of DMSO/water (9/1 v/v) containing LiBr 50 mM. The flow rate was 0.4 ml/min at 60°C. Samples were dissolved in the eluent at a concentration of 4 mg/ml for 1 h at 95°C, followed by 23 h at 40°C (Saake et al. 2001). Samples were filtered through regenerated cellulose membranes (0.45 μm). The percentage recovery after filtration, based on UV absorbance, was better than 75% in all cases. The molar masses were determined using a calibration with pullulan standards. Collection and calculation of the data was performed using WINGPC 4.6 software of Polymer Standard Service.

Enzymatic degradation and fractionation of GAX–DHP ZT polymerisation

Solutions of GAX ZT polymerisation were incubated with endo-β-1,4-xylanase solution (*Ecopulp* TX 200C; Röhm Enzym, Rajamäki Finland, SHARE 1031 7143). Enzyme was added at 200 nkat/g of GAX at 55°C for 1 h, under stirring. After treatment, the enzyme was inactivated by boiling at 100°C for 5 min. A reference solution of GAX/DHP (without enzyme) was treated under the same conditions. A precipitate was formed only with the xylanase treated sample and was collected by centrifugation. The supernatant was concentrated under reduced pressure to obtain the water-soluble fraction (W_{SOL}). The precipitate was poured into 95% aqueous dioxane and the supernatant and residue separated by centrifugation to obtain a dioxane-soluble fraction (D_{SOL}) and a residue, the dioxane-insoluble fraction (D_{INS}). All fractions were freeze-dried.

Sorption experiments of GAX to DHP

Sorption assays were performed in phosphate buffer (1/30 N; pH 5). GAX solutions were diluted to give a range of concentrations (0.025, 0.05, 0.1, 0.25, 0.5 and 1 mg/ml) from a stock solution of GAX prepared at 1 mg/ml. An aliquot of 1.5 ml was added to DHP samples (7.5 mg). GAX solutions and GAX DHP blends were incubated for 4 h at 25°C. After incubation, the samples were centrifuged at 7,700 *g* for 20 min. Unbound GAX present in the supernatant was quantified by HPAEC. The adsorbed GAX amounts were calculated from the difference between the GAX concentrations in the supernatant before and after adsorption. The DHP concentrations in the supernatant were determined from their absorbance at 280 nm. The supernatant solutions were then studied by fluorescence probe with pyrene.

Detection of hydrophobic microdomains by fluorescent probe

All spectra were recorded on a SPEX Fluoromax spectrophotometer (Edison, NJ, USA) equipped with thermostatic controlled cell at 25°C. A fixed amount of pyrene (1.6×10^{-6} M in the final solution) was added to the supernatant from the sorption experiments and samples, which were allowed to equilibrate overnight prior to fluorescence measurement. The samples were excited at 341 nm and emission spectra were recorded between 350 and 500 nm with a slit width of 1 mm for the excitation slit and 5 mm for emission. The relative intensity of peaks 1 (λ = 372 nm) and 3 (λ = 382 nm) was used to determine the local polarity of the medium surrounding the pyrene molecules.

Results

Dehydrogenative polymerisation of coniferyl alcohol in GAX solution by ZL and ZT methods

The polymerisations by ZT and ZL methods differed in the speed of reagent addition. In the ZL process all reactants were added simultaneously whereas in the ZT method they were added gradually (dropwise). The two methods therefore differed mainly in their distribution of radicals (and thus the associated QM) over the reaction time. Assuming the immediate oxidation of CA in the medium, the minute-by-minute distribution of QM throughout the reaction period was calculated for ZT and ZL according to the following equations:

$$[\mathrm{QM}]_{\mathrm{ZLt}} = [\mathrm{QM}]_{\mathrm{tot}} \mathrm{e}^{-kt}$$

$$[\mathrm{QM}]_{\mathrm{ZTt}} = [\mathrm{QM}]_{\mathrm{tot}}/14400 - [\mathrm{QM}]_{t-1} \mathrm{e}^{-kt}$$

where k is the observed rate constant of QM in water measured previously by Hemmingson and Leary (1.18×10^2 s^{-1}; Hemmingson and Leary 1975) and 14,400 s is the reaction time (Fig. 2).

Both reactions produced a colloidal suspension in the presence of GAX, in contrast to the reference polymerisation performed in phosphate buffer without GAX. This suggests an interaction between GAX and DHP. An effect of polysaccharide on DHP solubility had already been noted in the presence of pectin (Cathala and Monties

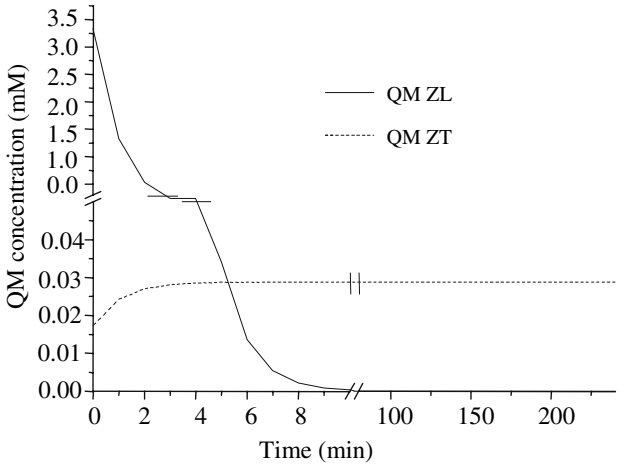

Fig. 2 Evolution of QM concentration during the ZL and ZT reactions. In the ZL reaction all the QM has reacted during the first minutes whereas in the ZT the level of QM remains low but constant all over the reaction. QM concentration is expressed as instantaneous concentration (i.e. concentration is calculate every minute)

2001). The possible formation of LCC in both syntheses was evaluated by SEC and NMR spectroscopy.

Size-exclusion chromatography (SEC) in dimethyl sulfoxide DMSO/water/lithium bromide in the ZT and ZL GAX reaction mixtures

DMSO containing 50 mM of LiBr at 60°C was used as solvent, since this mixture can solubilize both lignin and GAX and also dissociates most of the noncovalent interactions because of solvent polarity and the chaotropic effects of the lithium bromide combined with elution at high temperature. The SEC device was equipped with a differential refractive index (DRI) and ultraviolet (UV) detectors. The DRI is a universal detector which is sensitive to any kind of molecule dissolved in the solvent—in this case, polysaccharides and lignin—, whereas the UV system is specific to UV-absorbing materials, here DHPs. We confirmed that the noncovalent interactions between GAX and DHP were dissociated in our chromatographic system by first analysing a physical mixture (PM; mixture of GAX and ZL DHPs) obtained by suspending DHP in an aqueous GAX solution (Fig. 3a). After stirring, the suspension was freeze-dried, dissolved in DMSO/LiBr and injected into the SEC system. Two peaks were clearly distinguishable, the first (eluted around 22 ml) displayed a strong RI signal and hardly any UV absorption whereas the second (eluted around 28 ml) presented both UV and RI signals. Comparisons with pure standards confirmed that the peak at 22 ml corresponded to GAX and the other to the DHP fraction (data not shown). The evaluation of molar mass indicated an absence of significant variation in comparison with the starting materials and thus confirmed the ability of

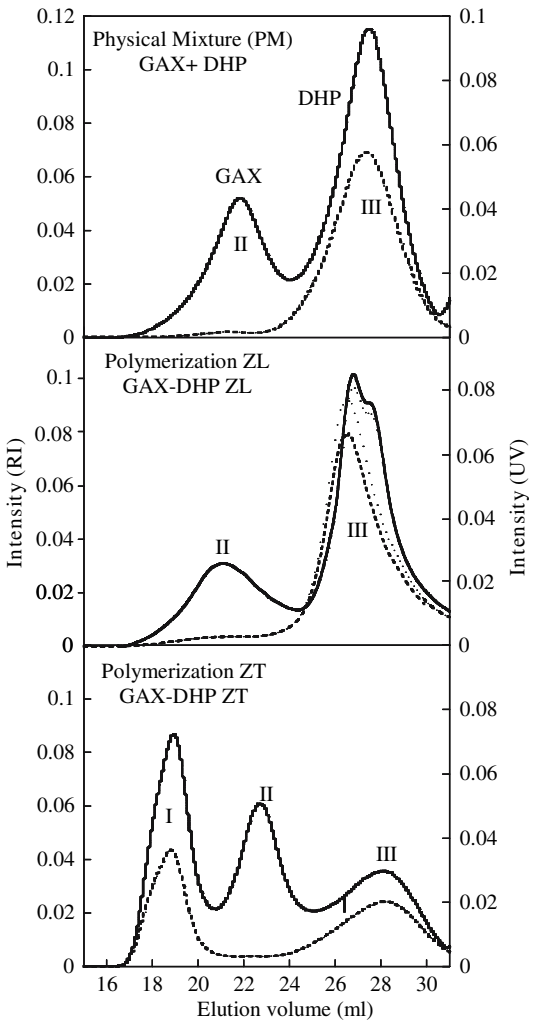

Fig. 3 a–c Elution profiles in DMSO of physical mixture (PM GAX + DHP **a**), GAX–DHP ZL product (polymerization ZL **b**) and GAX–DHP ZT (polymerization ZT **c**) (*filled line*), refractive index (RI signal); (*filled dot line*), absorbance at 280 nm (UV signal). The peak I (19 ml) occurs only in the ZT polymerization

our chromatographic system to limit DHP–GAX interactions. Two peaks, corresponding to GAX and DHPs, were again detected in the ZL experiments (Fig. 3b). However, careful examination of the molar mass revealed that the peak eluted around 22 ml presented a higher molar mass than pure GAX (Table 3) suggesting that some limited coupling may have occurred. This hypothesis was supported by the associated UV signal which also seemed to be more intense than in the PM profile. Three distinct populations were clearly visible in the case of GAX ZT (Fig. 3c). Peak I presented both UV and RI signals suggesting the presence of GAX and DHPs. The low elution volume (19 ml) indicated the presence of species with very large molar mass (Table 3) which could be attributed to covalent complexes between GAX and DHPs. This peak was absent from the PM and GAX–ZL profiles thus the

Table 3 Molar mass values of GAX-DHP ZT, GAX-DHP ZL and physical mixture (PM)

Product	GAX + DHP Physical mixture (PM)		GAX–DHP ZL Polymerization		GAX–DHP ZT Polymerization		
Peaks	II	III	II	III	I	II	III
Content (%)	49	51	48	52	36	37	27
Mw (g/mol) $\times 10^{-3}$	43	1.7	132	1.9	904	36	0.96

Mw Weight average molar mass equivalent to pullulan standards

hyphothesis of covalent complex occurring in this reaction can be proposed. This assumption is supported by the determination of the ratio between the RI and UV signals. The ratio measured for the peak eluted at 19 ml of the GAX–ZT reaction profiles is higher (2.45) compared to those measured in the peaks eluted around 28 ml in the physical mixture (1.66), the GAX–DHP ZL reaction (1.52) and the GAX–ZT reaction (1.7). This indicates the presence of nonabsorbing materials, i.e. xylans in the peak eluted at 19 ml. The second peak of the ZT elution curve was similar to that observed in the PM profile and corresponded to the GAX fraction. This hypothesis was supported by the low intensity of the UV signal, compared to the RI signal. Peak III had a larger elution volume (28 ml) and consisted of smaller molecular weight species that, according to their UV signal, could be attributed to DHP. It was concluded from this set of experiments that peak I observed in the ZT experiment could be attributed to a covalent complex that was not formed in the ZL experiment.

NMR analyses of ZT and ZL GAX–DHP

Solution-state ^{13}C NMR is a powerful method for revealing the structure of soluble lignin fragments. However, the presence of carbohydrates in the same spectra together with the low abundance of some linkages such as LCC, obscure the signals. Thus, one strategy usually reported in literature, consist in the use of ^{13}C labelled lignin monomers to increase the sensitivity of the analysis. This was used both in the case of synthetic (Parkas et al. 2001) and natural lignin (Terashima et al. 2002) and also applied to the investigation of LCC (Xi et al. 2000). Solution state ^{13}C NMR spectra of the ZL and ZT GAX–DHPs reaction obtained from α labelled coniferyl alcohol are reported in Fig. 4a and b. The peaks that can be discerned in the ZL–GAX ^{13}C-enriched DHPs were assigned according to Parkas et al. (2001; Fig. 4a; Table 4). Signals around 73 ppm (peaks noted **5**) can be assigned to the Cα in the aryglycerol-*β*-aryl ether structures. Cα in *β*–*β* structures can be attributed to the signals occurring around 86 ppm (peak noted **2**) and close to the *β*-5 linkages (88 ppm, peak **1**). Another signal arises at 83.5 ppm which can be assigned to the dibenzodioxocin linkages. Cα in *β*-*O*-4/α-*O*–R (R can be a polysaccharide or a phenol) structures are expected to have an intermediate chemical shift around 80–82 ppm (peaks **3 + 4**). Only a minor peak can be seen in this region for the ZL spectra. The general pattern of the ZT spectra is similar to the ZL one. However, all the signals are broader displaying a lower resolution. The other main modification concerns the region between 80 and 84 ppm that displays a very broad and irresolute signal while the peaks at 81 and 83.5 observed in the ZL spectra are not anymore visible. Broadening of the signal likely reflects the higher molar mass of the ZT sample compared

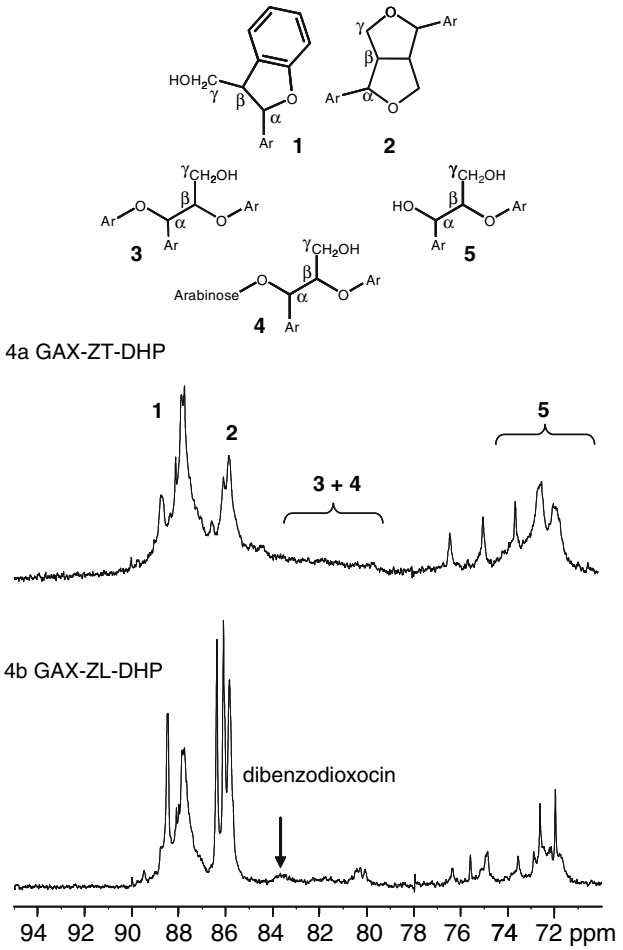

Fig. 4 Liquid ^{13}C NMR spectra of GAX–ZL–DHPs (**a**) and GAX–ZT–DHPs (**b**) obtained from α^{13}C labelled coniferyl alcohol

Table 4 Chemical shifts and relative bond frequencies for α carbon (expressed as relative percentages) of GAX–ZL–DHPs and GAX–ZT–DHPs synthesized with α^{13}C coniferyl alcohol

Chemical shifts (ppm)	Structural units	GAX–ZT–DHPs (%)	GAX–ZL–DHPs (%)	DHPs control [a] (%)
71–73 **(5)**	Cα in *β-O*-4 bonds + Cα esterified to carbohydrates	26.5	19.2	16
81 **(3 + 4)**	Cα etherified (carbohydrates or DHPs)	15.25	8.9	9
85 **(2)**	Cα in *β–β* bonds	14.9	18.2	25
87–88 **(1)**	Cα in *β*-5 bonds	23.15	29.15	30
130	Cα in coniferyl alcohol end groups	20.2	24.6	21

For spectral identification from 1 to 5, see Fig. 5

[a] Values obtained for control DHPs from reference Cathala et al. (2005)

to the ZL one. However, even whithout a high resolution, a signal in this range obviously occurs in the ZT spectra in contrast to the ZL spectra, thus suggesting the presence of peaks in the range of etherified Cα carbon with carbohydrate and phenol groups. A definitive attribution of this signal was attempted using a long-range correlation (HMQC; Ralph et al. 1999) between the H5 of arabinose and the 81–82 ppm signal region. Due to the large broadening of the signal, no correlation was detected. This extreme broadening can be explained by a very low mobility of the molecules that is consistent with the entrapment of the LCC linkages within a covalent network. This assumption is supported by the poor solubility of the ZT samples in the solvent (DMSO) at the NMR concentration range (i.e. 10–50 mg/0.5 ml). Indeed a gel like structure was formed in the tube even after acetylation. In order to deeper investigate the high-molar fraction that is almost insoluble under the NMR experimental conditions, samples were analysed by solid-state ^{13}C NMR analysis. Spectra of the ZL and ZT GAX mixture are presented in the Fig. 5a and b. The general pattern of the peaks was similar to that assigned in liquid-state except for the 81 ppm region (peak noted **3 + 4**) that displays a higher signal. Linkage frequencies and their relative contribution were obtained by the decomposition of the complex ZT and ZL spectra, followed by the estimation of their relative frequency (see Fig. 5 for the decomposition and Table 4 for the relative areas). The relative area of the peak at 81 ppm is roughly two times higher in the ZT (15.25%) than in the ZL experiment (8.9%; Table 4). As few changes of its half-width were observed, this increase was related to a higher proportion of linkages resonating at 81 ppm. Occurrence of a peak at 81 ppm in the ZL samples can be explained by the addition of some polysaccharides to the QM as suspected in SEC and also by the addition of phenol groups of DHPs. Indeed, the ZL methods is known to produce higher free phenol groups that are thought to react at acidic pH with quinone methide (Sipilä and Brunow 1991). The relative area measured in the ZL reaction mixture is in good agreement with previous studies done on bacterial cellulose/DHPs (9%) and bacterial cellulose/pectin/DHPs (6%) composites (Cathala et al. 2005) where it was concluded that bacterial cellulose based composites were almost free of LCC. Thus the increased on the intensity of the peak at 81 ppm in the ZT reaction mixture has to be

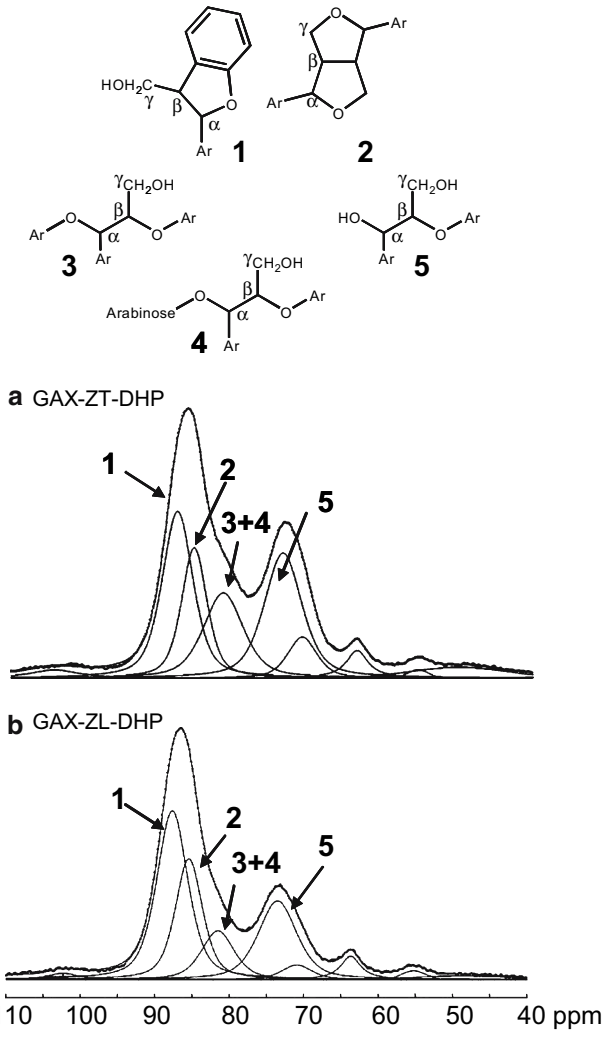

Fig. 5 Solid state ^{13}C NMR spectra of GAX–ZL–DHPs (**a**) and GAX–ZT–DHPs (**b**) obtained from α^{13}C labelled coniferyl alcohol

related to the formation of benzyl ether groups on the α carbon of DHPs. It has also to be noted that the proportion of the other type of linkages supports the idea of the modification of the monomer reactivity in the ZT reaction (Table 4). The amount of *β-O*-4 linkages (noted **5** in Fig. 5) increases while the condensed linkages (*β–β*, noted **2** and *β*-5, noted **1**) decrease together with residual coniferyl end groups. Accordingly, the structure of the GAX–ZT–DHPs is closer to those of natural lignin than GAX–ZL–DHPs.

Isolation of the LCC fraction by xylanase treatment and fractionation from the GAX–ZT reaction

Many techniques, involving chemical or enzymatic and/or organosolvent treatments have been used to isolate LCC (Koshijima et al. 1972; Takahashi and Koshijima 1987; Koshijima and Takahashi 1988). Avoiding a harsh procedure, the GAX ZT reaction was digested by an endoxylanase. Endo-*β*-1,4-xylanase randomly cleaves the xylane main chain and generates various substituted xylooligosaccharides. The GAX–ZT reaction product gave rise to a precipitate during the enzyme treatment, which was not observed in the absence of xylanase. The xylanase-treated sample was centrifuged and the supernatant freeze dried to give a water soluble fraction (W_{sol}). The precipitate was treated with a dioxan/water mixture to separate the dioxan/water soluble fraction (D_{sol}) from the dioxan/water insoluble fraction (D_{ins}). When these W_{sol} and D_{sol} fractions were analysed by ^{13}C NMR and SEC in DMSO/water LiBr, they mostly consisted of polysaccharides and DHP, respectively, (data not shown). D_{ins} could not be subjected to DMSO/water SEC- and NMR analyses due to its complete insolubility. However, the carbohydrate and lignin compositions of all fractions were determined. The results are reported in Table 5. Carbohydrate content decreased gradually between W_{sol} and the D_{ins} fraction, whereas a reverse relationship was observed for lignin content. The main variation concerned the molar ratios of arabinose and xylose. The D_{ins} fraction had a significantly higher arabinose content than the other fractions (Table 5), which indicated an enrichment of polysaccharides with high arabinose substitution in this fraction. These results are consistent with the ^{13}C NMR analysis and with previous works that demonstrated a covalent bond between the hydroxyl group of the C5 arabinose substituent and the α-position of the lignin monomer. No substantial differences in neutral or acid sugars could be detected in any fractions, in agreement with NMR data and despite previously reported results (Sipilä and Brunow 1991).

Sorption of GAX to ZL and ZT DHPs

Noncovalent interactions between GAX and DHPs were evaluated by testing the binding capacity of GAX on DHPs. Since DHPs are mostly insoluble in aqueous solutions, GAX solutions at various concentrations were incubated in the presence of a fixed quantity of DHP (Fig. 6). The amounts of GAX in the supernatant after centrifugation (Fig. 7) were determined by HPAEC after acid hydrolysis. The quantities of adsorbed materials (Fig. 7) were obtained from the difference between the amounts determined in binding assays and the starting solutions. ZT and ZL DHP presented very similar behavior for all the parameters investigated. Evolution of the arabinose/xylose ratio of the adsorbed materials was also monitored and any significant variation detected. All the ratios were similar to those of the total samples (roughly equal to 0.23). Thus there is no specific interaction with rich arabinose fraction of GAX.

Some DHPs were solubilized during the sorption experiment as evidenced by the increased UV absorbance measured in the supernatant after centrifugation. This ‘‘cosolvent effect’’ is reminiscent of the fact that ZL and ZT DHPs do not precipitate during synthesis. However, the amounts of soluble DHPs in the sorption experiment remained low (less than 1.5% of the total DHP) compared with the ZT and ZL experiments where all the DHPs was dispersed in the reaction medium.

Table 5 Carbohydrates and DHP content in fractions extracted after the xylanase treatment of GAX–DHP ZT product

Product	GAX–DHP ZT Polymerization	W_{SOL}	D_{SOL}	D_{INS}
Carbohydrates content (%)	50 (100)[a]	97.9 (82)[a]	24 (11)[a]	11 (7)[a]
Neutral sugars (%)	94.1 ± 0.4	93.7 ± 1.4	96.3 ± 0.7	95.5 ± 0.1
Acid sugars (%)	5.9 ± 1.0	6.3 ± 1.1	3.7 ± 0.2	4.5 ± 0.5
Ara/Xyl	0.23 ± 0.01	0.22 ± 0.02	0.24 ± 0.01	0.31 ± 0.02
Lignin content (%)	50 (100)[b]	2.1 (2)[b]	76 (34)[b]	89 (46)[b]

W_{SOL} Water soluble fraction, D_{SOL} dioxane soluble fraction, D_{INS} dioxane insoluble fraction, *Ara/Xyl* molar ratio of L-arabinose to D-xylose

[a] and [b], % yields of carbohydrates and lignin, respectively on the basis of original GAX–DHP ZT product

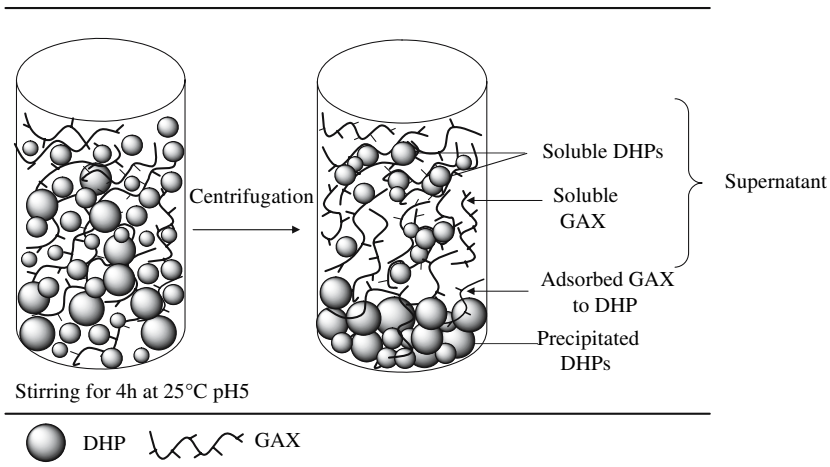

Fig. 6 Principle of sorption of GAX to DHP. Insoluble DHPs are mixed with GAX after 4 h stirring, the mixture is centrifuged. Amounts of DHPs solubilized and polysaccharides orbed were determined

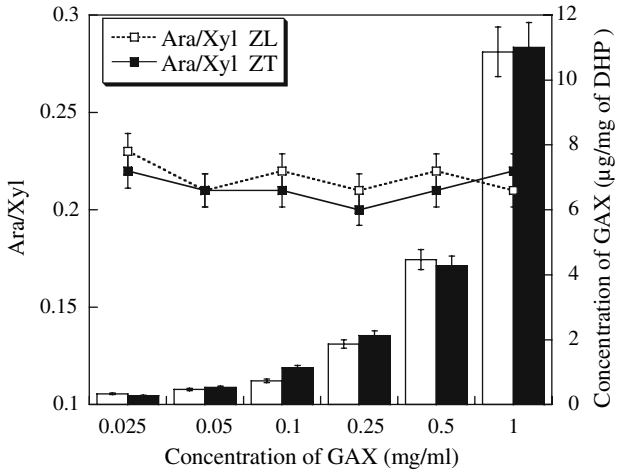

Fig. 7 Adsorption isotherms from GAX to DHPs. Experiments were performed with 7.5 mg of DHP and different GAX concentrations at 25°C, pH 5.0 for 4 h

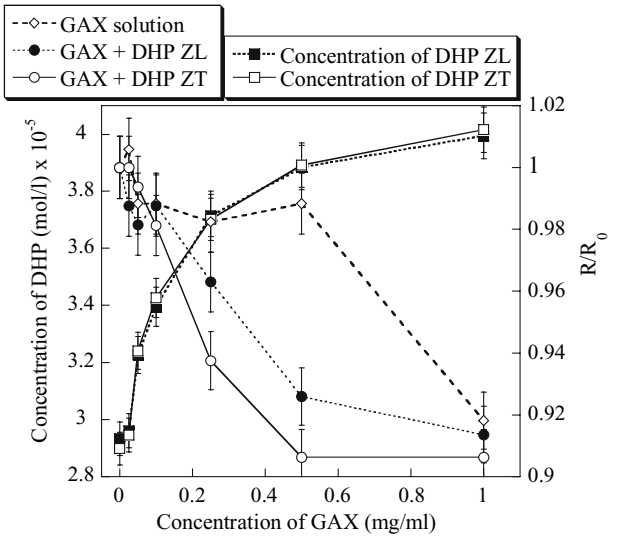

Fig. 8 Concentration of soluble DHPs (mol/l) and evolution of R/R_0 ratio in the supernatants of sorption experiments as a function of the total GAX concentration used for the sorption experiments

Formation of hydrophobic microdomains in the supernatant of sorption experiment solutions

Fluorescence properties of many molecules depend on the physicochemical characteristics of their environment. Pyrene is a hydrophobic molecule that has a fine fluorescence spectrum. The relative intensities of bands 1 (372 nm) and 3 (382 nm) are sensitive to the local polarity of the medium (I_1/I_3 = 1.7 in water and I_1/I_3 = 0.60 in hexane; Kalyanasundaram and Thomas 1997). This (I_1/I_3) ratio decreases as the polarity of the pyrene environment decreases (Winnik and Regismond 1996). Pyrene, due to its hydrophobic character, will be preferentially located in hydrophobic microdomains when they occur, so the curve of I_1/I_3 versus polymer concentration can be used to determine the formation of such domains. Another method consists of plotting the R/R_0 values versus GAX concentration for the GAX solution and supernatant from the sorption experiment where R_0 corresponds to the I_1/I_3 ratio at [GAX] = 0 mg/ml and R to the I_1/I_3 ratio at 0.025, 0.05, 0.1, 0.25 and 0.5 mg/ml of GAX. When R/R_0 is equal to 1 there is no formation of hydrophobic domains, whereas a decrease in the R/R_0 value indicates their formation. Dilute GAX solutions display a constant value of 1 (Fig. 8) whereas aggregation occurs at a high concentration (1 g/l). Thus it is likely that the GAX molecules exist as mostly nonassociated chains below this value. This pattern of aggregation, in polysaccharides forming hydrophobic domains, has already been reported for hemicellulose (Shigematsu et al. 1994a). The R/R_0 ratio, in the supernatant from the DHPs sorption experiments, was almost constant at very low concentrations and decreased to less than 0.1 g/l of GAX which was significantly lower than the aggregation limit of the pure GAX solution. No striking variation was noted between ZT and ZL DHPs. These results show

that DHPs and GAX are associated in a hydrophobic complex resulting in a decrease in local polarity and an increase in the soluble DHPs fraction. This pattern is reminiscent of previous studies that demonstrated the occurrence of condensed aggregates formed between DHPs and polysaccharides (Lairez et al. 2005).

Discussion

Formation of LCC in ZL and ZT polymerisation

The precise chemical mechanism responsible for LCC formation can be described as the nucleophilic addition of functional groups of polyosides to the transient quinone methide generated during dehydrogenative coupling of monolignols. The rates of addition of nucleophiles to quinone methides are reported to be pH dependent and linked to the dissociation constant of the hydroxyl compounds (Sipilä 1990). In the present study, the pH values in the ZL and ZT procedures were identical and the concentrations of hydroxyl compounds (GAX and water) were kept constant throughout the reaction time. Thus it can be assumed that the rate constants of addition of hydroxyl compounds to the QM were identical under both ZT and ZL conditions. The ZL and ZT methods generated roughly the same amount of QM. The amount of QM could in fact be estimated from the *β-O*-4 content of the final product, that is 15% of the total linkages for the ZT reaction and 12% for the ZL procedure (Cathala et al. 1998). The main difference between the two methods was the distribution of QM over the reaction time (Fig. 2). In the ZL process, all the CA was added at the beginning of the reaction. Assuming that peroxidase was not limiting, the amount of peroxidase (5 mg of 250–330 unit/mg) used in both experiments was able to oxidize 25 mM of CA per second whereas the total amount of CA added was 0.55 mM. Thus all the CA was immediately oxidized and produced a peak concentration of QM ($[QM]_{max}$ = 3.3 mM). Based on the rate constant of water addition determined by Leary (1972), it was calculated that almost all the QM reacted within 8 min (Fig. 2). In the ZT process CA was added throughout the reaction and the QM concentration attained a steady state of 2.9×10^{-5} M after roughly 3 min which lasted until the end of the reaction time. In both cases, the water concentration (55 M) predominated over the GAX concentration (3.12×10^{-2} M equivalent of monosaccharide).

The rate of LCC formation is a function of the concentration of the reactive species (i e. GAX and QM) and the rate constant of addition and can theoretically be described by the following equation:

$$[\mathrm{LCC}] = k_{\mathrm{GAX}}[\mathrm{GAX}][\mathrm{QM}] - k_{\mathrm{H_2O}}[\mathrm{H_2O}][\mathrm{QM}]$$

where k_{GAX} and k_{H_2O} are the rate constants of GAX and H_2O addition, respectively.

It is obvious from this equation that LCC formation is disfavoured in dilute aqueous solutions as high water concentrations can limit the reaction. If LCC formation occurs, it can be attributed either to a higher reactivity of the polysaccharides (i.e. high rate constant of addition) or to a modification of the local reaction conditions that then reduce the local water concentration and thus enhance polysaccharide addition. This situation can be summarized as follows:

(1) The rate constant of xylan addition is far higher than the rate constant of water addition. LCC formation will occur with both ZT and ZL methods.
(2) The rate constant of xylan addition is in the same order of magnitude as the rate constant of water addition and the local organization of the polymer has no impact on reactivity. Water addition will predominate and LCC will not be formed under ZL or ZT conditions.
(3) The rate constants of water and GAX addition are similar and the local organization of the polymer may favour the addition of polysaccharides. The longer addition time and gradual polymerisation of DHP will provide more opportunities for the polymers to reorganize and interact. LCC will be formed mainly during the ZT process.

Thus, independently of the rate constants of addition, comparison of the ZT and ZL reaction products provides a means of evaluating the competition between water and a polysaccharide and investigating the potential relevance of non covalent interactions in LCC formation.

Characterization of LCC in the ZL and ZT reactions

The characterization of LCC is not an easy task, since these low frequency linkages are diluted in highly complex lignin/polysaccharide structures. In order to demonstrate the difference existing between ZT and ZL, without any ambiguity, we characterized both the polymeric effects (i.e. formation of high molar mass complexes by SEC) and the molecular attributes of the LCC formation (i.e. identification of the covalent bonding by NMR).

Size exclusion chromatography (SEC) is a powerful technique for studying the macromolecular properties and characteristics of polymers. However, artefacts are usual and aggregation, for example, can be a source of considerable misinterpretation as already emphasized in previous studies (Porsch and Sundelöf 1994; Saake et al. 2001; Cathala et al. 2003). For these reasons, we used DMSO/water containing 50 mM of LiBr at 60°C, a system suitable for the analysis of both polysaccharides and lignin or DHP. The set of SEC experiments demonstrated that the ZT method had a marked impact on LCC formation since high

molar mass complexes were exclusively observed in this process although some limited coupling could occur in the ZL reaction (increase of peak II molar mass in Fig. 3 and Table 3). The SEC investigation of physical mixtures of DHP and GAX proved that even after drying of the physical mixtures the aggregation observed in aqueous system (Fig. 7) could be fully re-dissolved in the DMSO/water eluent (Fig. 3a). This strongly supports the conclusion, that the high molar mass products found in the ZT synthesis are really covalently bound LCC.

These conclusions were confirmed by NMR studies which demonstrated covalent linkages between GAX and ZT–DHP involving the arabinose moiety of GAX. This was further confirmed by analysing the D_{ins} fraction that was enriched in arabinose compared to the starting samples. The role of arabinose in LCC formation has already been evidenced both in model and cell wall materials (Takahashi et al. 1982; Ohnishi et al. 1992; Toikka et al. 1998). More surprising was the absence of glucuronic acid enrichment in the D_{ins} fraction and the lack of proof in the NMR data of the occurrence of an ester linkage between glucuronic acid and the α carbon of the lignin monomer. Indeed this addition was suggested to be prevalent at neutral pH in previous work by Sipilä (1990). However, the addition of carboxylic acid was carried out in mixed organic/water solutions with monomeric models (Sipilä and Brunow 1991). This difference in experimental conditions may have resulted in the different reactivities of the active groups. However, another point linked to our experimental conditions might be responsible for these different findings. Indeed, as discussed above, the formation of covalent bonds is linked to the occurrence of hydrophobic clusters. Such clusters might reject polar glucuronic acid groups thereby limiting their reactivity. Further investigations under a range of experimental conditions are needed to discuss this point in detail.

It can be concluded that the formation of covalent linkages occurs between GAX and DHP by addition of the C_5 hydroxyl groups of the arabinose of the quinone methide generated during the ZT dehydrogenating process. This does not happen in the ZL reaction although all the reaction parameters are identical except for the QM concentration over the reaction time. To get an in-depth understanding of the process, the interactions between GAX and DHPs were then evaluated by physico-chemical means.

Evidence for noncovalent interaction between DHPs and GAX

Sorption experiments provide a simple but efficient means of demonstrating noncovalent interactions between soluble and insoluble components. In the present study, interactions between DHPs and GAX were evidenced and compared to similar values obtained in studies of hemicellulose/cellulose interaction. The degree of GAX bonding, with both DHPs, attained roughly 10 μg/g and was thus in the same range as observed between cellulose and polysaccharides in similar conditions. Indeed, the amounts of xyloglucans adsorbed to cellulose were about 14 μg/mg, whereas values of 2.5 and 4 μg/mg were measured for arabinan and galactan-rich pectins, respectively (Vincken et al. 1995; Zykwinska et al. 2005). The main difference between the present results and these earlier ones is related to the fact that the DHP/GAX isotherm did not attain a plateau, at least in the range of concentrations studied here. In previous studies, the plateau of adsorption isotherms has been attributed to full coverage of the accessible surfaces of the cellulose molecules. This is supported by the fact that the plateau values vary according to the type of cellulose (Hayashi et al. 1987). In the present study, the absence of a plateau together with the shape of the isotherm (exponential evolution) may indicate that the accessible surfaces became more and more abundant with the increase in GAX concentration suggesting that the GAX molecules were able to disrupt insoluble DHP aggregates and thus increase the accessible surfaces. This assumption is consistent with the increase in DHPs concentration observed in the supernatants after centrifugation (Fig. 8). In the case of a [GAX]/[DHP] ratio of 1/7.5 (mg/mg), for example, the DHP concentration was about 1.5-fold higher in the presence of GAX compared to the water blank (Fig. 8). This indicates the existence of an attractive interaction between GAX and DHP. Such a finding has been previously reported and evidenced for other kinds of polysaccharides (Higuchi et al. 1971; Shigematsu et al. 1994b; Cathala and Monties 2001). The pattern of interaction did not vary significantly between ZL and ZT DHPs. However, it should be remembered that the ZT and ZL DHPs only presented small structural differences (Cathala et al. 1998). Indeed they exhibited rather similar β-*O*-4 and hydroxyl group contents, and small differences in molar mass. This is an advantage when comparing the addition rate constants for the two methods as explained below. However, it is not the most favourable system for detecting the specificity of noncovalent interactions between GAX and different lignin types. Closer analysis of this specificity would necessitate the presence of large structural differences and accordingly a variety of different lignins and lignin models. This will require further investigation in the future. Our main conclusion is that both DHPs interact with GAX.

Noncovalent interactions and end-wise process promote the formation of covalent coupling

The present works demonstrate the occurrence noncovalent interactions between DHP and GAX molecules. However,

interactions occurred with both types of DHPs whereas LCC were mainly formed during the ZT reaction. The absence of LCC formation in the ZL reaction can be explained by the fact that CA reacts almost immediately and simultaneously to the colloid formation. Since ZL DHPs and xylans can interact, aggregates are likely formed explaining the formation colloidal suspension that limit the precipitation of the ZL DHPs. Since all the CA molecules react rapidly the reaction is stopped before any process of rearrangement (aggregates fusion, DHPs diffusion, etc). In the case of the ZT process, formation of aggregates also occurs at the early times of the reaction. Since CA and DHPs are rather hydrophobic molecules (Shigematsu et al. 1994b), during the addition process, they will be likely located and polymerized within aggregates formed earlier in the reaction process. This will increases the local DHPs concentration as previously evidenced (Lairez et al. 2005) inducing dehydration process by self aggregation. Elimination of water molecules will promote the addition of GAX. Noncovalent interactions together with the slow addition process result in the building up of supramolecular structures that induced a change in reactivity. However it is clear that without one of these two parameters, LCC will not be efficiently formed. *In planta*, the dehydration process has already been observed during lignification (Inomana et al. 1992) whereas formation of xylan–lignin network was also suggested by Salmen and Olsson (1998). Similar behaviour to that described here can occur and affect the reactivity of lignin-like molecules, as it will favour addition of the hydroxyl group of polysaccharides to quinone methide by lowering the local water concentration within the complexes. Thus in complement to the previously described hypotheses (high polysaccharide concentration, long reaction time), we propose a general scheme of LCC formation based on the formation of aggregates by noncovalent interaction. This favours the nucleophilic addition of hemicellulose to QM by increasing the polysaccharide and/or lowering the local water concentrations, and thus limits water competition (Fig. 9).

Conclusion

Based on the results of model experiments some new features in the process of LCC formation are proposed. Lignin-like products were shown to interact with GAX to form hydrophobic complexes. As summarized in Fig. 9, this led to dehydration of the local environment around the lignin-like growing chains, thereby limiting the addition of water to the quinone methide formed during polymerisation. In the present study, arabinose was found to provide the most reactive nucleophile whereas no such evidence was found with glucuronic acid addition.

We therefore propose that local noncovalent interactions influence and control the formation of covalent linkages between lignin and carbohydrate networks by forming supramolecular assemblies. To understand how this control proceeds, the specific relationships and interactions between different lignin and xylan types needs to be investigated. However, the model proposed in Fig. 9 can be generally applied to cell wall formation. It implies that LCC formation increases throughout the lignification process together with the lignin content. This suggests that LCC formation is maximal at the end of lignification and

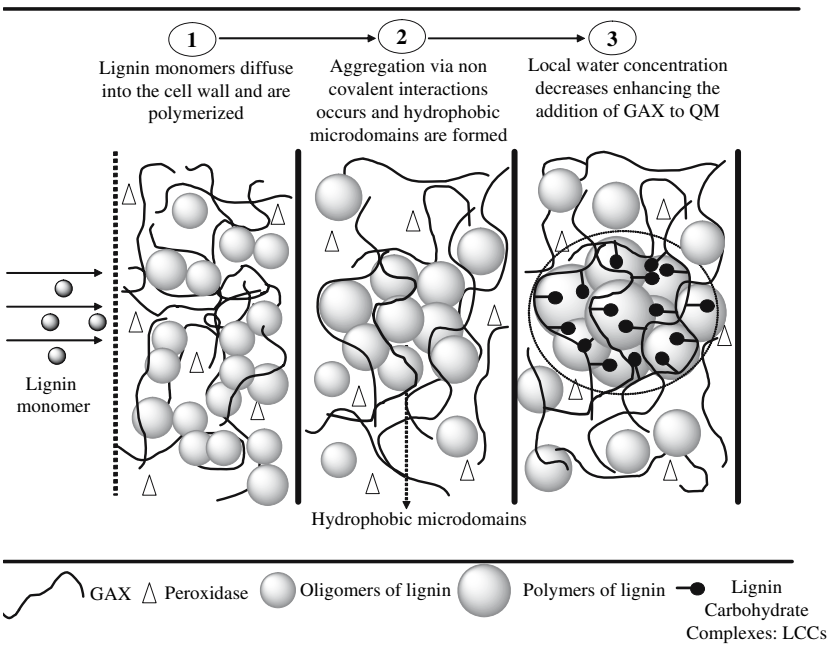

Fig. 9 Schematic representation of the formation of LCC during the lignification process

that this process can be understood as the final step in cell wall construction by blockage of the interpenetrating networks. This process can thus be considered as a regulation mechanism in addition to the oxidative pathway that dominates at the earlier stages of cell wall construction.

Acknowledgments Access to the NMR facilities of the BIBS platform (Biopolymers, Interactions, Structural Biology) of INRA-Nantes was greatly appreciated by the authors.

References

Björkman A (1957) Studies on finely divided wood. Part 3. Extraction of lignin–carbohydrate complexes with neutral solvents. Svensk Papperstidning 60:158–159

Cathala B, Monties B (2001) Influence of pectins on the solubility and the molar mass distribution of dehydrogenative polymers (DHPs, lignin model compounds). Int J Biol Macromol 29:45–51

Cathala B, Saake B, Faix O, Monties B (1998) Evaluation of the reproducibility of the synthesis of dehydrogenation polymer models of lignin. Pol Deg Stab 59:65–69

Cathala B, Saake B, Faix O, Monties B (2003) Association behaviour of lignins and lignin model compounds studied by multidetector size-exclusion chromatography. J Chrom A 1020:229–239

Cathala B, Rondeau-Mouro C, Lairez D, Bedos-belval B, Durand H, Gorrichon L, Touzel JP, Chabbert B, Monties B (2005) Models systems for the understanding of lignified plant cell wall formation. Plant Biosyst 139:93–97

Fry SC (1986) Cross-linking of matrix polymers in the growing cell walls of angiosperms. Annu Rev Plant Physiol 37:165–186

Grabber JH, Ralph J, Hatfield RD (2000) Cross-linking of maize walls by ferulate dimerization and incorporation into lignin. J Agric Food Chem 48:6106–6113

Grabber J, Ralph J, Hatfield RD (2002) Model studies of ferulate-coniferyl-alcohol cross-product formation in primary maize walls: implications for lignification in grasses. J Agric Food Chem 50:6008–6016

Hayashi K, Mardsen M, Delmar D (1987) Pea xyloglucan and cellulose: xyloglucan–cellulose interactions in vitro and in vivo. Plant Physiol 83:384–389

Hemmingson J, Leary G (1975) The chemistry of reactive lignin intermediates. Part II. Addition reactions of vinyl-substituted quinone methides in aqueous solution. J Chem Soc Perkin II:1584–1587

Higuchi T, Ogino K, Tanahashi M (1971) Effect of polysaccharides on dehydropolymerization of coniferyl alcohol. Wood Res 51:1–11

Inomana F, Takabe K, Saiki H (1992) Cell wall formation of conifer tracheid as revealed by rapid-freeze and substitution method. J Electron Microsc 41:369–374

Kalyanasundaram K, Thomas JK (1997) Environmental effects on vibronic band intensities in pyren monomer fluorescence and their application in studies of micellar systems. J Am Chem Soc 99:2039–2044

Koshijima T, Taniguchi T, Tanaka R (1972) Lignin carbohydrate complex. Holzforschung 26:211–218

Kuhlmann KF, Grant DM (1968) The nuclear overhauser enhancement of the carbon-13 magnetic resonnance spectrum of formic acid. J Am Chem Soc 90:7355–7357

Koshijima T, Takahashi N (1988) Molecular properties of lignin–carbohydrate complexes from beech (*Fagus crenata*) and pine (*Pinus densiflora*) woods. Wood Sci Technol 22:177–189

Lairez D, Cathala B, Monties B, Bedos-Belval F, Duran D, Gorrichon L (2005) On the first steps of lignification: aggregation during coniferyl alcohol polymerisation in pectin solution. Biomacromolecules 6:763–774

Leary G (1972) The chemistry of reactive lignin intermediates. Part I. Transients in coniferyl alcohol photolysis. J Chem Soc Perkin II 5:640–642

Ludley FH, Ralph J (1996) Improved preparation of coniferyl and sinapyl alcohols. J Agric Food Chem 44:2942–2943

Ohnishi J, Watanabe N, Koshijima T (1992) Synthesis of dehydrogenation polymer–polyoside complexes by peroxidase. Phytochemistry 31:1185–1190

Parkas J, Paulsson M, Westermark U, Terashima N (2001) Solid state NMR analysis of β-^{13}C-enriched lignocellulosic material during light-induced yellowing. Holzforschnung 55:276–282

Porsch B, Sundelöf L (1994) Size exclusion chromatography and dynamic light scattering of dextrans in water: explanation of ion-exclusion behaviour. J Chrom A 669:21–30

Ralph J, Marita JM, Ralph SA, Hatfield RD, Lu F, Ede R, Peng J, Quideau S, Helm RF, Grabber JH, Kim H, Jimenez-Monteon G, Zhang Y, Jung H-JG, Landucci L, MacKay JJ, Sederoff RR, Chapple C, Boudet AM (1999) Solution-state NMR of lignins. In: Argyropoulos DS, Rials T (eds) Advances in lignocellulosics characterization. TAPPI, Atlanta, pp 55–108

Saake B, Kruse T, Puls J (2001) Investigation on molar mass, solubility and enzymatic fragmentation of xylans by multi-detected SEC chromatography. Biores Technol 80:195–204

Salmen L, Olsson AM (1998) Interaction between hemicelluloses, lignin and cellulose: structure-property relationships. J Pulp Pap Sci 24:99–103

Shigematsu M, Goto A, Yoshida S, Tanahashi M, Shinoda Y (1994a) Hydrophobic regions of hemicellulose estimated by fluorescent probe method. Mokuzai Gakkaishi 11:1214–1218

Shigematsu M, Goto A, Yoshida S, Tanashi M, Shinoda Y (1994b) Affinities of monolignols and saccharides determined by the solubility method. Mokuzai Gakkaishi 40:321–327

Sipilä J (1990) On the reactions of quinone methide intermediates during lignin biosynthesis: a study with models compounds. Ph.D thesis, Department of chemistry, University of Helsinki

Sipilä J, Brunow G (1991) On the mechanism of formation of non-cyclic benzyl ether during lignin biosynthesis. Part 4. The reactions of a β-*O*-4 type quinone methide with carboxylic acids in the presence of phenol. The formation and stability of benzyl esters between lignin and carbohydrate. Holzforschung 45:9–14

Takahashi N. Koshijima T (1987) Properties of enzyme-unhydrolyzable residue of lignin–carbohydrate complexes isolated from Beech Wood. Wood Res 74:1–11

Takahashi N, Koshijima T (1988) Ester linkages between lignin and glucuronoxylan in a lignin–carbohydrate complex from beech (*Fagus crenata*) wood. Wood Sci Technol 22:231–241

Takahashi N, Azuma J, Koshijima T (1982) Fractionation of lignin–carbohydrate complexes by hydrophobic-interaction chromatography. Carbohydr Res 107:161–168

Tanaka K, Nakatsubo F, Higuchi T (1976) Reactions of guaiacylglycerol-β-guaiacyl ether with several sugars I. Reactions of quinone methide with D-glucuronic acid. Mokuzai Gakkaishi 22:589–590

Terashima N (2001) Possible approaches for studying three dimensional structure of lignin. In: Moroshi N, Komamine A (eds) Molecular breeding of woody plants. Elsevier, Amsterdam, pp 257–261

Terashima N, Fukushima K, He L-F, Takabe K (1993) Comprehensive model of the lignified plant cell wall. In: Jung HG, Buxton DR, Hatfield RD, Ralph J (eds) Forage cell wall structure and digestibility. Amer Soc Agronomy, Madison, pp 247–270

Terashima N, Ralph SA, Landucci LL (1996) New facile syntheses of monolignols glucosides; *p*-glucocoumaryl alcohol coniferin and syringin. Holzforschung 50:151–155

Terashima N, Hafren J, Westermark U, Vanderhart DL (2002) Non destructive analysis of lignin by NMR spectroscopy of specifically ^{13}C-enriched lignins. Holzforschung 56:43–50

Toikka M, Sipila J, Teleman A, Brunow G (1998) Lignin–carbohydrate model compounds. Formation of lignin methyl arabinoside and lignin methyl galactoside benzyl ethers via quinone methide intermediates. J Chem Soc Perkin Trans 1:3813–3818

Vincken JP, Keizer A, Beldman G, Voragen G (1995) Fractionnation of xyloglucans fragments and their interactions with cellulose. Plant Physiol 108:1579–1585

Winnik F, Regismond ST (1996) Fluorescence methods in the study of the interactions of surfactants polymers. Colloids Surf A Physicochem Eng Asp 118:1–39

Winter H, Barakat A, Cathala B, Saake B (2006) Preparation of arabinoxylan and its sorption on bacterial cellulose during cultivation. In: Fisher K, Heinze T (eds) Makromolecular symposium series: hemicelluloses. Wiley, Weinheim, pp 85–92

Xi Y, Yasuda S, Wu H, Liu H (2000) Analysis of the structure of lignin–carbohydrate complexes by the specific ^{13}C tracer method. J Wood Sci 46:130–136

Zykwinska AW, Ralet MCJ, Garnier CD, Thibault JFJ (2005) Evidence for in vitro binding of pectin side chains to cellulose. Plant Physiol 139:397–407